ESTIMATION OF SOIL MOISTURE USING SENTINEL-1 AND SENTINEL-2 IMAGES

R. Esmaeili Sarteshnizi[1], S. Sahebi Vayghan[2*], I. Jazirian[3]

[1] Department of Surveying Engineering, Marand Technical College, University of Tabriz, Tabriz, Iran - Rouhollahesmaili77@gmail.com
[2] Department of Remote Sensing and GIS, Kharazmi University, Tehran, Iran - saiedehsahebi@yahoo.com
[3] Geodesy and Geomatics Engineering Faculty, University of K.N. Toosi (KNTU), Tehran, Iran - jazirian@kntu.ac.ir

Commission IV, WG IV/3

KEY WORDS: Soil Moisture, Sentinel-1, Sentinel-2, Gaussian, Laplacian, Majority, Morphology, Rank

ABSTRACT:

Soil moisture is a vital parameter for environmental research such as agriculture, hydrology, natural resources, environmental hazards, etc. It is essential to have timely soil moisture maps prepared with high accuracy, speed, and low cost. Therefore, in this study, an attempt was made to evaluate the efficiency of Sentinel 1 and 2 sensor images in some cases to prepare a soil moisture map. For this study, soil moisture was sampled at 24 points in the common area of the two images in the south of Malard city, Tehran province (Iran) was obtained by survey. After pre-processing the images, the values of bands 1 to 7, 11, and 12 of the Sentinel-2 and applying filters (Gaussian, Laplacian, Majority, Morphology, and rank) to the Sentinel-1 soil moisture were calculated. Moreover, R, R2, and RMSE were calculated using soil moisture obtained from sample points. Furthermore, Maps of data used by sentinel-1 and sentinel-2 images were obtained. Using maps of data shows the potential of applied filters to sentinel-1 and bands used for sentinel-2 in the estimation of soil moisture. According to the results, the highest coefficient of determination (R2) for the Sentinel-2 is related to band 6 with 84%. The result of Sentinel-1 demonstrated that the highest coefficient of determination was related to the Rank filter (54%). The highest correlation of the Sentinel-2 and the Sentinel-1 is related to band 6 with 74% and the Rank filter with 46%, respectively. The lowest RMSE in Sentinel-2 and Sentinel-1 is related to band three (1.64 %) and rank filter (1.03 %), respectively. According to the obtained results, band 6 in the Sentinel-2 and filter in Sentinel-1 have better performance among the data and methods used. However, it is emphasized that using more samples can be tested for improving results.

1. INTRODUCTION

Soil moisture is the heart of the earth's system (Dorigo et al., 2017), affecting the variability of evapotranspiration, runoff, and energy fluxes by affecting the water and energy input cycle on earth (Seneviratne et al., 2010). Similarly, excess or deficiency of soil moisture can lead to floods or droughts(Brocca et al., 2011; Dorigo et al., 2017; Koster et al., 2010; Wang et al., 2011). Soil moisture is of great importance in engineering, agricultural, geological, environmental, biological, and hydrological studies of soil mass (SU et al., 2014). Furthermore, soil moisture is a significant property of agriculture, which affects the dissolution and transfer of nutrients and microbial activity in the soil(Deng et al., 2020; Fares and Alva, 2000; Kim et al., 2008; Vellidis et al., 2008).

Climatic data on soil moisture are essential for improving our understanding of the long-term dynamics of water, energy, and carbon cycles on Earth (Dorigo et al., 2017). In-situ observations of soil moisture and vegetation variables are vital factors for validating land surface models and satellite-derived products (Zhang et al., 2017). Due to the crisis in continuous measurements of soil moisture in terms of spatial and temporal and costly and time-consuming field measurements, it is practically impractical to do so, especially in impassable, mountainous, and large areas. Optics remote sensing includes the visible, near-infrared, and mid-infrared spectral. In this system, images are produced by recording reflected radiation of the sun from the earth by satellite sensors. Various studies have been performed to determine soil moisture(Babaeian et al., 2016; Sadeghi et al., 2017; Tian and Philpot, 2015; Whiting et al., 2004; Zhang and Zhou, 2016).

The development of microwave remote sensing resulting from the Sentinel operational satellite launching has increased the accuracy of soil moisture estimation at higher spatial and temporal resolution (Singh et al., 2020). In the last two decades, the ability of microwave remote sensing to determine the dielectric properties of soil based on the amount of surface emission has led to the estimation of soil moisture (Mohanty et al., 2017). Different frequencies (X, C, and L bands) are commonly used to detect soil moisture (Calvet et al., 2010). Soil reflection in the L band through soil ductility strongly affects soil moisture in the 2-3 cm of the first soil layer (Fernandez-Moran et al., 2017). Various approaches have been proposed in the recent 35 years based on microwave remote sensing (Awe et al., 2015; Chen et al., 2012; Zhang and Zhou, 2016). Since the 1980s, several surface scattering models have been developed for passive microwave remote sensing (Sun et al., 2015), including Kirchhoff models, which consist of the geometrical optics model (GOM) (Ulaby et al., 1986), the physical optical model (POM) (Ulaby et al., 1986) he small perturbation model (SPM) (Ulaby et al., 1986), the integral equation model (IEM) (Fung et al., 1992), the advanced integral equation model (AIEM) (Chen et al., 2003, 2000), Q / H model (Choudhury et al., 1979; Wang and Choudhury, 1981) and Qp model (Shi et al., 2005) for the bare soil area (Zhang and Zhou, 2016). In 2020 Sing et al. evaluated the potential of Sentinel-1A satellite images to estimate soil moisture in a semi-arid region by using 37 soil samples and measuring the soil moisture from 5 cm below the ground surface using ML3 theta probe(Singh et al., 2020). The authors, after processing of Sentinel-1A images, applied modified Dubois model to calculate the relative permittivity of the soil from the backscatter values (σ°) and calculate the volumetric soil moisture at each pixel by applying the universal Topp's model accord with the measured values with RMSE = 0.035 and R = 0.75. This approach provides a first-order soil moisture estimation from Sentinel-1A images in sparsely vegetated agricultural land(Singh et al., 2020). Foucras et al. in 2020, have estimated the surface soil moisture at a spatial resolution of 500 m and a temporal resolution of at least 6 days by combining Sentinel-1 and

Sentinel-2 and MODIS images using change detection technique over a three-year period. The output from the presented SMES algorithm "Soil Moisture Estimations from the Synergy of Sentinel-1 and optical sensors (SMES)" by the authors is a moisture index ranging between 0 and 1, with 0 corresponding to the driest soils and 1 to the wettest soils is well correlated with RMSE below 6 vol%, for the African regions in particular (Foucras et al., 2020). (Ranjbar and Akhoondzadeh, 2021), have estimated the volumetric moisture of the soil surface using support vector regression (SVR) and perceptron artificial multilayer neural network (ANN-MLP) by Sentinel-1 and Sentinel-2 data. Estimation of soil surface volumetric moisture by support vector regression method using Sentinel 1 image has the best accuracy, and estimation of this parameter by ANN-MLP method using Sentinel 2 image has the worst accuracy. Calculating the square of the correlation coefficient has demonstrated that the best and worst correlation coefficients are related to the Sentinel 1 image using the backup vector and the Sentinel 2 image using the ANN-MLP method. The lowest and highest root mean square error is related to the support vector regression method with Sentinel 1 image and the perceptron multilayer artificial neural network method with Sentinel 2 image, respectively (Ranjbar and Akhoondzadeh, 2021).
(Fallah, 2013), has estimated soil moisture using satellite images of MODIS, ETM sensors, and SWAP model that the correlation coefficient was measured between values equal to 76%. (Ranjbar and Akhoondzadeh, 2020), have obtained the soil moisture using SVR and ANN methods in the Sentinel 1 and 2 satellite images with correlation coefficients of 0,659 for Sentinel 1 image with support vector regression method and 0,409 For Sentinel 2 image with multi-layer perceptron of artificial neural network method.
This research seeks to find and model the relationship between satellite imagery data and soil moisture so that soil moisture can be estimated at different levels and provide access to remote or inaccessible places. However, various research has been conducted in the field of soil moisture evaluation using optical and radar satellite images, the purpose of this research is to evaluate the efficiency of bands 1 to 7, 11, and 12 of the Sentinel-2 and apply filters (the Gaussian, Laplacian, Majority, Morphology, and rank) to the Sentinel-1 for evaluation of soil moisture.

2. AREA OF STUDY

The study area is related to the south and southeast of Malard city in Tehran province. Malard city is adjacent to Ferdis in the north, Joqin village in the south, Shahriyar in the east and Mahdasht in the west. The longitude and latitude of the geometric center of Malard County is 35.6649 ° N, 50.9826 ° E. In this study, 24 points in the south and southeast of Malard County were sampled to estimate soil moisture, shown in figure 1 and the two polytheistic areas (Sentinel-1 and Sentinel-2).

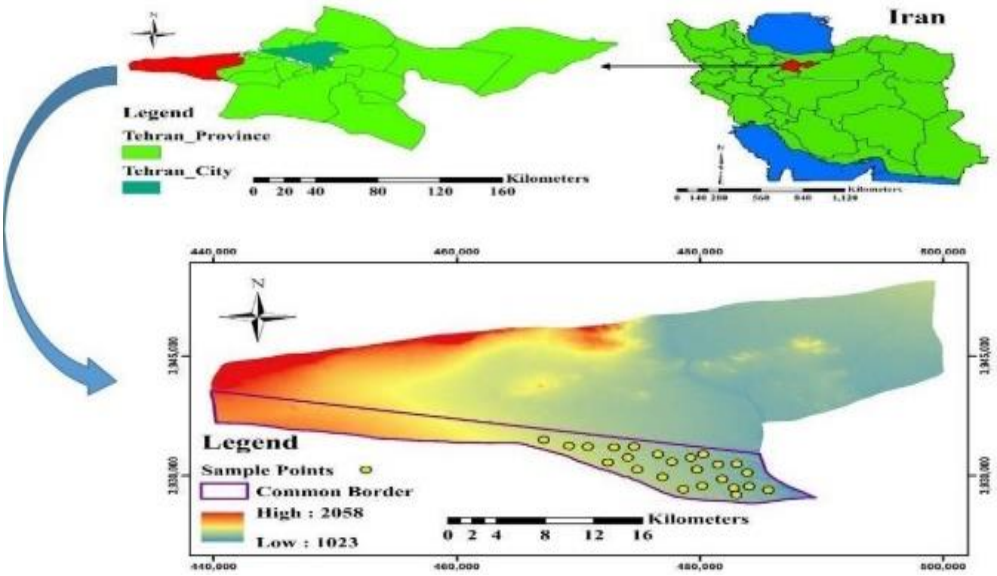

Figure 1. Study area.

3. DATA AND METHODS

Ground data: A total of 24 points were obtained by random field sampling. The reason for choosing this method is to find areas with low vegetation or no vegetation where the soil moisture changes in the high range. The moisture of the topsoil (depth 0 to 5 cm) was measured by the direct weighting method in the laboratory. Sampling was performed on 27/02/2020 when the satellite passed through the area. Also, the coordinates of the sampling points were taken by GPS. The samples' moisture has been measured with high accuracy in several steps and repetitions in the laboratory by the oven device.

4. METHOD OF OBTAINING 100% SOIL MOISTURE

Soil moisture is expressed as a percentage of its dry weight and is defined as relationship (1):

$$\omega = \frac{w_1 - w_2}{w_2} * 100, \quad (1)$$

Where ω= Soil moisture
W1 = Wet soil weight (g)
W2 = dry weight of soil (g)

As part of the European Space Agency's program "Copernicus", Sentinel-1A and Sentinel-1B were launched (in April 2014 and April 2016, respectively) for observation and monitoring of the

Earth's surface and providing operational applications with environmental information (Foucras et al., 2020). Different weather conditions are ineffective on Synthetic Aperture Radars (SARs) and acquire data at any time of the day or night (Foucras et al., 2020). Single and dual-polarization images in the C-band with the wavelength of approximately 6 cm are provided by the SAR payloads which are positioned 180° apart in a sun-synchronous orbital plane (Foucras et al., 2020). Sentinel-1, a synthetic aperture radar(SAR) sensor that implements C-band imaging (Torres et al., 2012). Sentinel-2 has been developed by the European Space Agency (ESA) for land monitoring, including a constellation of two multi-spectral imaging satellites, Sentinel-2A (S-2A), launched in June 2015 and Sentinel-2B (S-2B), launched in March 2017 (Foucras et al., 2020). It provides global coverage of the Earth's land surface with a revisit frequency of 5 (Foucras et al., 2020). It provides global coverage of the Earth's land surface with a revisit frequency of 5 (Foucras et al., 2020). The images are in 13 spectral bands, consist of visible and mid-infrared wavelengths, at three various spatial resolutions, including 10, 20, and 60 m (Foucras et al., 2020).
In this study, the authors compared the efficiency of the Sentinel-1 image as a radar sensor and the Sentinel-2 image as an optical sensor in estimating soil moisture. Moreover, the spatial resolution of the used bands is 10 and 20 meters (bands 1 to 8, 11, and 12). First, geometric and radiometric corrections were applied to satellite images. Then, to evaluate the capability of Sentinel-2 sensor images, the values of bands 1 to 8, 11, and 12 (in the sampled points) with the moisture content of the sample points were analyzed. To evaluate the capability of the Sentinel-1 sensor, the value of the band at VH polarization and some filters applied to the images, including Gaussian, Laplacian, Majority, Morphology, and rank filters, have been used. To evaluate the capability of each of the items used, linear regression (R),

$$Y_i = f(x_i, \beta) + e_i, \quad (2)$$

Where Yi = dependent variable
F =function
xi = independent variable
β = unknown parameters
ei = error terms
Determination coefficient (R2)

$$R2 = 1- (RSS / TSS), \quad (3)$$

Where R2 = Coefficient of determination
RSS = Sum of squares of residuals
TSS = Total sum of squares
And RMSE was used

$$RMSE = \sqrt{(\frac{1}{n}\sum_{i=1}^{n}(pridict - Ground)^2}, \quad (4)$$

Where N = equal to the total number of data
Predict = equal to the value predicted by the model
Ground = the amount of ground data

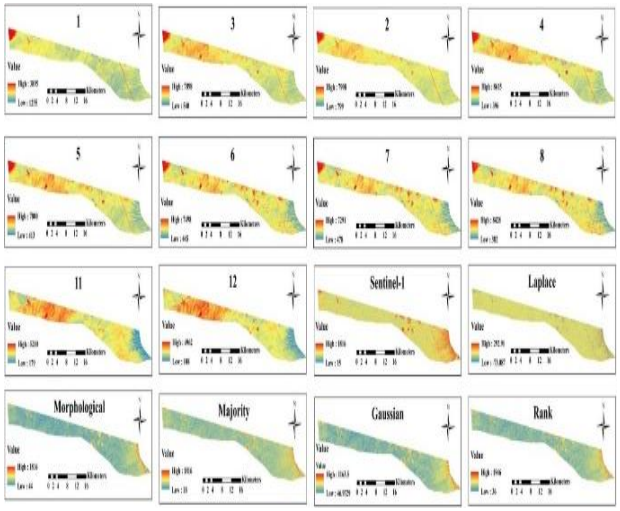

Figure 2. Map of the data used.

The graph of determination coefficients (R2) and line equation (regression formula) of the data used were obtained. Figure 3 is variable models used and a graph of the coefficient of determination of Sentinel2 bands in the next step, which is provided in table 2. According to the models used in figure3, y is the dependent variable for each band of Sentinel-2, and x is the soil moisture percentage obtained using each band of sentinel-2.

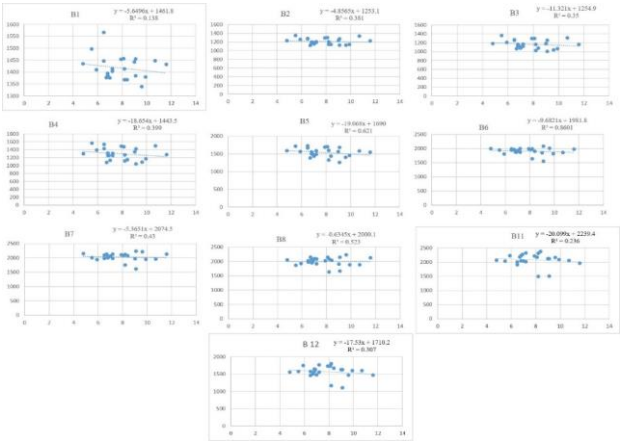

Figure 3. diagram of the coefficient of determination of Sentinel-2 sensor bands.

Table1 demonstrates that the lowest coefficient of determination is related to band one with a soil moisture value of 8.70%, which indicates the fragile relationship of this band with soil moisture. Nonetheless, the most powerful relationship with soil moisture among the other bands belongs to band 6, with 86% of the coefficient of determination. After band 6, bands 5, 8, and 7 have a high coefficient of determinations, with 62.1%, 52.3%, and 43%, respectively. Therefore, these bands have a strong relationship. with soil moisture, so using these bands in determining soil moisture is useful.

Number of Bands	R^2 (%)	Soil Moisture(%)
Band 1	13.8	8.70
Band 2	38.1	8.09
Band 3	35	7.93
Band 4	39.9	8.29
Band 5	62.1	8.16
Band 6	86.01	8.097
Band 7	43	8.096
Band 8	52.3	7.98
Band 11	23.6	8.15
Band 12	30.7	8.1

Table 1. coefficient of determination for each band in Sentinel-2.

Figure 4 demonstrates the coefficients of determination and the line equation for the radar data used (Sentinel-1). This figure illustrates the coefficient diagram for the initial sentinel-1 image and the Gaussian, Laplacian, Majority, morphological, and Rank filters. As can be seen in figure4, y is the dependent variable for each filter used for Sentinel-1, and x is the Soil moisture percentage obtained using filters. Further, these values have been provided for better review in Table 2.

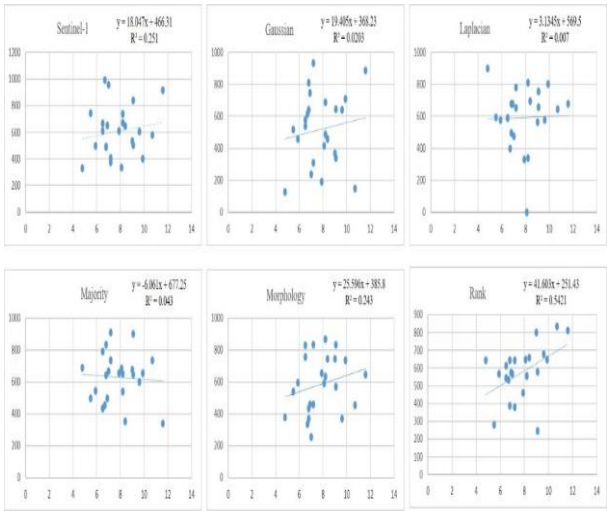

Figure 4. Sentinel-1 sensor product determination coefficient diagram.

As can be seen in Table 2, the Laplacian, Gaussian, and Majority filters have the lowest coefficient of determination with values of 0.7%, 2.03%, and 4.3%, respectively, which indicate the fragile relationship of this band with soil moisture. Nonetheless, the Rank filter, with a coefficient of determination of 54.21%, has a robust relationship with soil moisture compared to the other filters. The determination coefficient diagram and equation of the Sentinel-1 raw image line show that the determination coefficient is equal to about 25%, indicating a weak relationship between soil moisture and sentinel-1 image data.

Filters	R^2 (%)	Soil Moisture (%)
No filters	25.1	8.19
Gaussian	2.03	8.69
Laplacian	0.7	8.92
Majority	4.3	7.99
morphological	24.3	8.33
Rank	54.21	7.89

Table 2. coefficient of determination for each filters in Sentinel-1.

Table 3 indicates the correlation, RMSE, and soil moisture values obtained results between the input data (sentinel-2 image bands, sentinel-1 image bands, and filters applied to the sentinel-1 image) and soil moisture.

Data	RMSE	R	Soil Moisture Values (%)
B1	11.42	0.13	8.70
B2	3.68	0.2	8.09
B3	1.64	0.306	7.93
B4	6.16	0.315	8.29
B5	4.5	0.67	8.16
B6	3.68	0.74	8.097
B7	3.67	0.369	8.096
B8	2.26	0.415	7.98
B11	4.4	0.16	8.15
B12	4.88	0.19	8.19
Sentinel-1	4.92	0.18	8.19
Gaussian	11.34	0.15	8.69
Laplacian	14.29	0.068	8.92
Major	2.36	0.069	7.99
Rank	1.03	0.46	7.89
Morphology	6.67	0.13	8.33

Table 3. Correlation and RMSE results between input data and soil moisture.

According to this table, the highest correlation coefficient in the Sentinel-2 image is related to band 6 with a soil moisture value of 8.097% and band 5 with a soil moisture value of 8.16%. The lowest error rate was related to band 3 with a soil moisture value of 7.93%. Concerning the Sentinel-1 image, the highest correlation coefficient and the lowest error were related to the Rank filter with soil moisture values of 7.89%.

5. CONCLUSION

Providing a timely map of soil moisture at high speed and low cost is significant for managers and researchers in various fields. In recent years, remote sensing researchers have been seeking to develop methods based on satellite image processing to obtain more accurate soil moisture maps. However, given the multiplicity of satellite sensors and the methods used, new researches are always required. In this research, the efficiency of

Sentinel-1 and Sentinel-2 images in estimating soil moisture has been investigated. The results obtained from regression, coefficient of determination and RMSE, demonstrate the highest coefficient of determination (R2) is related to band 6 of Sentinel-2 sensors with 84%. In the Sentinel-1 sensor, the highest coefficient of determination is related to the Rank filter (54%).
In the correlation regression (R) section, the highest correlation of Sentinel-2 was related to band 6 with 74%, and in Sentinel-1 sensor, the highest correlation was with a filter with 46%.
In the correlation regression (R) section, the highest correlation of Sentinel-2 was related to band 6 with 74%, and in the Sentinel-1 sensor, the highest correlation was with a filter with 46%. The lowest error was related to band three (1.64) in Sentinel-2, and the lowest error was related to filter (1.03) in Sentinel-2.
Based on the results of this study, in the Sentinel-1 sensor, the Rank filter had the best potential, and in the Sentinel-2 sensor, band 6 had the best potential. Results of this research demonstrate that band 6 of the Sentinel 2 image and the rank filter in the Sentinel 1 image have a more significant relationship with soil surface moisture. Moreover, the filter and band mentioned are more sensitive in evaluating soil surface moisture than other Sentinel-2 bands and the filters used in Sentinel-1. In this study, the ground data as soil moisture data was measured by the direct weighting method in the laboratory, and the average soil moisture in the area was obtained at 7.81%. With the comparison of the soil moisture measured using Sentinel-1 and Sentinel-2 images with Ground data, low values of RMSE show the high efficiency of the sentinel-1 and sentinel-2 images in the assessment of soil moisture. Nevertheless, the points that should be mentioned are for image processing, and it is better to use images at different times and do more processing, and also for more definite comments, more sample points, as well as more research, should be made.

REFERENCES

Awe, G.O., Reichert, J.M., Timm, L.C., Wendroth, O.O., 2015. Temporal processes of soil water status in a sugarcane field under residue management. *Plant Soil*. 387, 395–411.

Babaeian, E., Homaee, M., Montzka, C., Vereecken, H., Norouzi, A.A., van Genuchten, M.T., 2016. Soil moisture prediction of bare soil profiles using diffuse spectral reflectance information and vadose zone flow modeling. *Remote Sens. Environ*. 187, 218–229.

Brocca, L., Moramarco, T., Melone, F., Wagner, W., Hasenauer, S., Hahn, S., 2011. Assimilation of surface-and root-zone ASCAT soil g products into rainfall–runoff modeling. IEEE Trans. *Geosci. Remote Sens*. 50, 2542–2555.

Calvet, J.-C., Wigneron, J.-P., Walker, J., Karbou, F., Chanzy, A., Albergel, C., 2010. Sensitivity of passive microwave observations to soil moisture and vegetation water content: L-band to W-band. IEEE Trans. *Geosci. Remote Sens*. 49, 1190–1199.

Chen, K.-S., Wu, T.-D., Tsang, L., Li, Q., Shi, J., Fung, A.K., 2003. Emission of rough surfaces calculated by the integral equation method with comparison to three-dimensional moment method simulations. IEEE Trans. *Geosci. Remote Sens*. 41, 90-101.

Chen, K.-S., Wu, T.-D., Tsay, M.-K., Fung, A.K., 2000. Note on the multiple scattering in an IEM model. IEEE Trans. *Geosci. Remote Sens*. 38, 249–256.

Chen, X., Chen, S., Zhong, R., Su, Y., Liao, J., Li, D., Han, L., Li, Y., Li, X., 2012. A semi-empirical inversion model for assessing surface soil moisture using AMSR-E brightness temperatures. J. Hydrol. 456, 1–11.

Choudhury, B.J., Schmugge, T.J., Chang, A., Newton, R.W., 1979. Effect of surface roughness on the microwave emission from soils. J. Geophys. Res. Ocean. 84, 5699–5706.

Deng, X., Gu, H., Yang, L., Lyu, H., Cheng, Y., Pan, L., Fu, Z., Cui, L., Zhang, L., 2020. A method of electrical conductivity compensation in a low-cost soil moisture sensing measurement based on capacitance. *Measurement*. 150, 107052.

Dorigo, W., Wagner, W., Albergel, C., Albrecht, F., Balsamo, G., Brocca, L., Chung, D., Ertl, M., Forkel, M., Gruber, A., 2017. ESA CCI Soil Moisture for improved Earth system understanding: State-of-the art and future directions. *Remote Sens. Environ*. 203, 185–215.

Fares, A., Alva, A.K., 2000. Evaluation of capacitance probes for optimal irrigation of citrus through soil moisture monitoring in an entisol profile. *Irrig. Sci*. 19, 57–64.

Fernandez-Moran, R., Al-Yaari, A., Mialon, A., Mahmoodi, A., Al Bitar, A., De Lannoy, G., Rodriguez-Fernandez, N., Lopez-Baeza, E., Kerr, Y., Wigneron, J.-P., 2017. SMOS-IC: An alternative SMOS soil moisture and vegetation optical depth product. *Remote Sens.* 9, 457.

Foucras, M., Zribi, M., Albergel, C., Baghdadi, N., Calvet, J.-C., Pellarin, T., 2020. Estimating 500-m resolution soil moisture using Sentinel-1 and optical data synergy. *Water*. 12, 866.

Fung, A.K., Li, Z., Chen, K.-S., 1992. Backscattering from a randomly rough dielectric surface. *IEEE Trans. Geosci. Remote Sens*. 30, 356–369.

Fallah ,M. 2013. Estimation of Soil Moisture Using SWAP Agro-Hydrological Model and Comparison with Field and Satellite Measurement of Madis and TM Sensors, Faculty of Agriculture and Water Resources of Guilan University.

Kim, Y., Evans, R.G., Iversen, W.M., 2008. Remote sensing and control of an irrigation system using a distributed wireless sensor network. *IEEE Trans. Instrum. Meas.* 57, 1379–1387.

Koster, R.D., Mahanama, S.P.P., Livneh, B., Lettenmaier, D.P., Reichle, R.H., 2010. Skill in streamflow forecasts derived from large-scale estimates of soil moisture and snow. *Nat. Geosci*. 3, 613–616.

Mohanty, B.P., Cosh, M.H., Lakshmi, V., Montzka, C., 2017. Soil moisture remote sensing: *State-of-the-science. Vadose Zo. J*. 16, 1–9.

Ranjbar, S., Akhoondzadeh, M., 2021. Study of soil moisture change effects on L-band DInSAR phase. *Eng. J. Geospatial Inf. Technol*. 8, 81–101.

Ranjbar, S. and Akhoondzadeh, M., 2020. Volumetric soil moisture estimation using Sentinel 1 and 2 satellite images. *Engineering Journal of Geospatial Information Technology*. 7(4), pp.215-232.

Sadeghi, M., Babaeian, E., Tuller, M., Jones, S.B., 2017. The optical trapezoid model: A novel approach to remote sensing of

soil moisture applied to Sentinel-2 and Landsat-8 observations. Remote Sens. *Environ*. 198, 52–68.

Seneviratne, S.I., Corti, T., Davin, E.L., Hirschi, M., Jaeger, E.B., Lehner, I., Orlowsky, B., Teuling, A.J., 2010. Investigating soil moisture–climate interactions in a changing climate: *A review*. *Earth-Science Rev*. 99, 125–161.

Shi, J., Jiang, L., Zhang, L., Chen, K.S., Wigneron, J.-P., Chanzy, A., 2005. A parameterized multifrequency-polarization surface emission model. *IEEE Trans. Geosci. Remote Sens*. 43, 2831–2841.

Singh, A., Gaurav, K., Meena, G.K., Kumar, S., 2020. Estimation of soil moisture applying modified dubois model to Sentinel-1; a regional study from central India. *Remote Sens*. 12, 2266.
SU, S.L., Singh, D.N., Baghini, M.S., 2014. A critical review of soil moisture measurement. *Measurement*. 54, 92–105.

Sun, S., Che, T., Wang, Jian, Li, H., Hao, X., Wang, Z., Wang, Jie, 2015. Estimation and analysis of snow water equivalents based on C-band SAR data and field measurements. *Arctic, Antarct. Alp. Res*. 47, 313–326.

Tian, J., Philpot, W.D., 2015. Relationship between surface soil water content, evaporation rate, and water absorption band depths in SWIR reflectance spectra. *Remote Sens. Environ*. 169, 280–289.

Torres, R., Snoeij, P., Davidson, M., Bibby, D., Lokas, S., 2012. The Sentinel-1 mission and its application capabilities, in: 2012 IEEE International Geoscience and Remote Sensing Symposium. *IEEE*. 1703–1706.

Ulaby, F.T., Moore, R.K., Fung, A.K., 1986. Microwave remote sensing: Active and passive. Volume 3-From theory to applications.

Vellidis, G., Tucker, M., Perry, C., Kvien, C., Bednarz, C., 2008. A real-time wireless smart sensor array for scheduling irrigation. Comput. *Electron. Agric*. 61, 44–50.

Wang, A., Lettenmaier, D.P., Sheffield, J., 2011: Soil moisture drought in China, 1950–2006. J. *Clim*. 24, 3257–3271.

Wang, J.R., Choudhury, B.J., 1981. Remote sensing of soil moisture content, over bare field at 1.4 GHz frequency. J. Geophys. *Res. Ocean.* 86, 5277–5282.

Whiting, M.L., Li, L., Ustin, S.L., 2004. Predicting water content using Gaussian model on soil spectra. *Remote Sens. Environ*. 89, 535–552.

Zhang, D., Zhou, G., 2016. Estimation of soil moisture from optical and thermal remote sensing: *A review*. *Sensors* 16, 1308.

Zhang, S., Roussel, N., Boniface, K., Ha, M.C., Frappart, F., Darrozes, J., Baup, F., Calvet, J.-C., 2017. Use of reflected GNSS SNR data to retrieve either soil moisture or vegetation height from a wheat crop. *Hydrol. Earth Syst. Sci*. 21, 4767–4784.